Protonation and Stability of the Globular Domain of Influenza Virus Hemagglutinin

Qiang Huang,* Robert Opitz,* Ernst-Walter Knapp,† and Andreas Herrmann*
*Institute of Biology, Molecular Biophysics, Humboldt-Universität zu Berlin, 10115 Berlin, and †Institute of Chemistry, Crystallography, Freie Universität Berlin, 14195 Berlin, Germany

ABSTRACT A partial dissociation of the HA1 subunits of influenza virus hemagglutinin (HA) is considered to be the initial step of conformational changes of the HA ectodomain leading to a membrane fusion active conformation (L. Godley, J. Pfeifer, D. Steinhauer, B. Ely, G. Shaw, R. Kaufmann, E. Suchanek, C. Pabo, J. J. Skehel, D. C. Wiley, and S. Wharton, 1992, *Cell* 68:635–645; G. W. Kemble, D. L. Bodian, J. Rose, I. A. Wilson, and J. M. White, 1992, *J. Virol.* 66:4940–4950). Here, we explore a mechanism that provides an understanding of the physical and chemical basis for such dissociation and relies on two essential observations. First, based on the x-ray structure of HA from X31 (I. A. Wilson, J. J. Skehel, and D. C. Wiley, 1981, *Nature* 289:366–373), and by employing techniques of molecular modeling, we show that the protonation of the HA1 subunits is enhanced at the conditions known to trigger conformational changes of the HA ectodomain. Second, we found that the dependence of the calculated relative degree of protonation of the HA1 domain on temperature and pH is similar to that observed experimentally for the conformational change of HA assessed by proteinase K sensitivity. We suggest that at the pH-temperature conditions typical for the conformational change of HA and membrane fusion, dissociation of the HA1 subunits is caused by the enhanced protonation of the HA1 subunits leading to an increase in the positive net charge of these subunits and, in turn, to a weakened attraction between them.

INTRODUCTION

After endocytic uptake of an influenza virion, its membrane glycoprotein hemagglutinin (HA) mediates the fusion of the viral envelope with the endosomal membrane. Each monomer of the homotrimeric organized HA consists of two subunits, HA1 and HA2, which are linked by a single disulfide bond. The three-dimensional structure of the bromelain-cleaved ectodomain of HA (subtype H3) at neutral pH is known from x-ray crystallography at a resolution of 3 Å (Wilson et al., 1981). The first 20 amino acids of the N-terminus of HA2, the so-called fusion peptide, are located ~100 Å away from the distal part of the ectodomain and ~35 Å away from the viral membrane, oriented toward the trimer interface. The HA-mediated fusion is triggered by acidic pH (Maeda and Ohnishi, 1980; Huang et al., 1981; White et al., 1982), which causes the HA ectodomain to convert into a fusogenic conformation, thereby exposing the fusion peptide. X-ray crystallographic studies of a fragment of the ectodomain suggest that the loop of the HA2 subunit connecting two α-helical segments in the neutral form becomes part of an extended trimeric coiled coil at low pH (Bullough et al., 1994; Qiao et al., 1998; Chen et al., 1999). For a detailed discussion of the conformational change of HA see reviews of Ramalho-Santos and de Lima (1998) and of Eckert and Kim (2001).

Although the formation of the coiled-coil structure was observed after low pH treatment of a HA2 fragment (Bullough et al., 1994), previous studies on a synthetic peptide (Carr and Kim, 1993) and on HA2 expressed in bacteria in the absence of HA1 (Chen et al., 1995) have shown that the coiled-coil structure forms spontaneously at neutral pH as well. Thus, very likely, acidification may be required for another step of the conformational change of the HA ectodomain essential for the coiled-coil formation. To elucidate this pH-dependent structural change is mandatory to understand the pathway of conformational alterations and intermediates of the HA ectodomain leading to a fusion active state. In particular, a careful assessment of the role of low pH for the conformational change of HA will reveal why the coiled-coil formation of HA requires a low pH whereas those of other viral fusion-mediating proteins such as gp41/gp120 of HIV-1 do not.

Different approaches have suggested that a rearrangement of the HA1 globular (distal) domains of HA occurs at low pH and is required for formation of the fusion active conformation (Godley et al., 1992; Kemble et al., 1992; Böttcher et al., 1999). Locking the HA1 subunits by intermolecular disulfide bonds in the distal part prevented the conformational change of HA and abolished its fusion activity (Godley et al., 1992; Kemble et al., 1992). Thus, a sideward reorientation of the originally tightly associated monomers of HA1 globular domain, at least of their distal parts, seems to be essential for formation of the fusion active conformation of HA. An attractive hypothesis is that enhanced protonation of the solvent-exposed HA1 domain by lowering the pH destabilizes this domain, because the largest contribution to the electrostatic potential within a

Submitted August 14, 2001, and accepted for publication November 6, 2001.

Address reprint requests to Dr. Andreas Herrmann, Humboldt-Universität zu Berlin, Institute of Biology/Molecular Biophysics, Invalidenstrasse 43, D-10115 Berlin, Germany. Tel.: 49-30-2093-8830; Fax: 49-30-2093-8585; E-mail: Andreas.Herrmann@rz.hu-berlin.de.

0006-3495/02/02/1050/09 $2.00

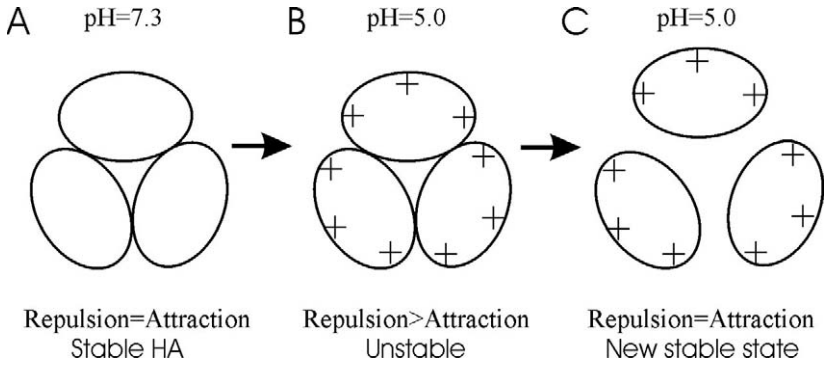

FIGURE 1 The partial dissociation of the HA1 domain induced by low pH. (*A*) Top view of the HA1 domain of the stable trimeric HA ectodomain at neutral pH; (*B*) Enhanced protonation of the solvent-exposed HA1 domain weakens the attraction between three HA1 subunits at low pH; (*C*) The new stable state of HA1 domain after its partial dissociation at low pH is determined by a balance between attractive and repulsive forces. For further details, see text.

protein arises from the protonatable amino acids that can carry a net charge.

In this study, we will elucidate whether enhanced protonation of globular HA1 domain at low pH can be responsible for a displacement of monomers in this domain. For this purpose, we employ complementarily the techniques of molecular modeling based on a continuum solvent model and an experimental approach to probe for the HA stability. Although a detailed simulation approach monitoring the relevance of protonation to the dynamics of proteins involving a large number of atoms is not feasible yet, the protonation pattern of proteins can be calculated with a continuum solvent model and Monte Carlo sampling techniques (Bashford and Karplus, 1991; Beroza et al., 1991; Ullmann and Knapp, 1999). On this basis, the thermodynamic probability of protonation of each titratable site in a protein can be evaluated. The protonation pattern depends on the number of titratable sites and their spatial localization in the protein as well as on the properties of the solvent medium, e.g., bulk pH and temperature. Calculations are based on the three-dimensional structure of the ectodomain of HA from strain X31 at neutral pH (Wilson et al., 1981). We will show that the dependence of the HA1 domain protonation on temperature and pH is similar to that of the conformational change of HA probed by proteinase K sensitivity. We surmise that protonation of titratable residues of the HA1 domain at low pH enhances the electrostatic repulsion between the monomers of the globular domain and thus lowers the stability of their association. Sideward relocation of the HA1 globular domains may enable the subsequent steps of conformational change of HA into a fusogenic state by a spring-loaded mechanism (Carr and Kim, 1993).

THEORY AND MODELING METHODS

Physical basis of destabilization of HA1 domain

To outline our hypothesis on the physical basis of the destabilization of HA1 domain caused by low pH, we have to emphasize two features of the crystal structure of the ectodomain in its nonfusogenic state at neutral pH (Wilson et al., 1981). First, because there is only one disulfide bond linking HA1 and HA2 polypeptide chains of a monomer, and no covalent bond between the monomers of the ectodomain, the tight assembly of monomers is due to noncovalent interactions between the monomers and solvent effects. Second, it is obvious that in an aqueous solvent, the solvent components (water, proton, other ions, etc.) can interact directly only with the surface of HA1 domain, whereas an essential part the of HA2 buried under the HA1 domain is shielded from such an interaction. This can be rationalized by calculation of the solvent-accessible surface of the protein. The difference in solvent accessibility is of consequence for protonation of the ectodomain at low pH. Protonation is a chemical reaction occurring between solvent-accessible titratable residues of the protein and the protons in aqueous solvent. Thus, initially, the protonation state of the HA1 domain should be influenced when decreasing the pH. Protonation of the HA2 subunits can take place only after a destabilization and rearrangement of the HA1 domain allowing access of the solvent to the HA2 subunits of a HA trimer.

Here, we will address the question of whether enhanced protonation at low pH can destabilize the HA1 domain of a trimer. To answer this, let us consider the consequences of low pH to the interactions essential for the stability of the HA ectodomain in its nonfusogenic conformation, which are the noncovalent interaction between HA monomers as well as solvent effects. When decreasing pH, the corresponding influence of aqueous solvent is the change of HA protonation state; namely, the average number of protons associated with the HA1 subunits by protonation becomes enhanced. With respect to the average number at neutral pH, the additional associated protons at low pH will alter the noncovalent interaction between HA monomers: the van der Waals and electrostatic forces. However, according to the nature of forces, in general, the van der Waals forces will be influenced very slightly by these additional associated protons, and their change can be neglected in comparison to that of the electrostatic force. The latter is strongly affected because protons possess net positive charge. Because the three subunits in the HA1 domain of the trimer are identical and at symmetric positions (Wilson et al., 1981), the protonation state at low pH is similar for each subunit. Taken together, 1) the protonation-induced net force is essentially of electrostatic nature and 2) the induced electrostatic force between the subunits by enhanced protonation is repulsive. We suggest that this repulsion triggers a destabilization and (partial) dissociation of the HA1 domain.

To describe the destabilization process, a simple model for the top view of the HA1 domain is shown in Fig. 1. At neutral pH (Fig. 1 *A*), ignoring the locally thermal vibrations of atoms, the HA ectodomain can be viewed as a stationary, force-balanced structure. This means the overall forces between the monomers must be zero; i.e., all attractive contributions and

repulsive contributions to the forces cancel. Of course, the stability of a protein conformation is also related to other factors as well, e.g., solvent interaction. When decreasing the pH, an additional repulsive force (the above-mentioned induced net force essentially of electrostatic nature) between three HA1 monomers is introduced. Because the (original) attractive forces cannot cancel the increased repulsion, the structure becomes force unbalanced. From the viewpoint of molecular interaction, it is equivalent to consider that the attraction among the HA1 monomers is weakened. Thus, the three HA1 monomers will come apart. The new positions of the three HA1 subunits will be determined by a new balance between attractive and repulsive forces depending on the atomic coordinates; i.e., the extent of the dissociation depends on the changes in attractive and repulsive forces with respect to the dissociation state itself. Thus, a partial or even a full dissociation will be triggered (see the Fig. 1 *B* and *C*). Although the actual pattern might be more complicated, its nature will be the same as that illustrated in Fig. 1. Based on the above-mentioned experiments (e.g., Böttcher et al., 1999), we consider the dissociation as partial.

Generating all-hydrogen-atoms structures

Calculations were done for the ectodomain of HA from influenza virus X31 (subtype H3). The coordinates of the non-hydrogen atoms were taken from the crystal structure in Protein Data Bank (PDB code 2HMG). All-hydrogen-atoms structures were generated by using the HBUILD command of program CHARMM (Brooks et al., 1983) with the force field of CHARMM22 (MacKerell et al., 1998), assuming their usual protonation state at pH 7. The positions of the hydrogen atoms were optimized by energy minimization by fixing all non-hydrogen atoms at their positions determined from the crystal structure. For the energy minimization, water molecules were not considered, and the dielectric constant was set to $\epsilon = 1$ everywhere. Noncovalent interactions were calculated with an atom-based cutoff radius of 13 Å. The structures with all-hydrogen atoms were obtained by performing 1000 steps of energy minimization with the step descent method, followed by 500 steps with the conjugate gradient method. With this procedure, we generated the atomic coordinates for the trimeric HA1 domain, for a single HA1 chain, and for the HA2 domain. In computations, we ignore a few of residues that are located proximal to the part of the ectodomain close to the viral membrane, which are not crucial at all for the structures of HA1 domain and HA2 domain and the contact between the HA1 and HA2 subunits. Therefore, the residues 16–328 and 1–134 of the HA1 and HA2 chains, respectively, were considered.

Protonation calculation

The protonation state of a titratable site j in a protein can be characterized by a parameter x_j, whose value is 1 for the protonated state and 0 for the unprotonated state (Bashford and Karplus, 1991; Ullmann and Knapp, 1999). The protonation state of the protein with N titratable sites is characterized by the N-component vector: $\mathbf{x} = (x_1, \ldots, x_j, \ldots, x_N)$. The total number of possible protonation states is 2^N. The protonation probability θ_j (or protonation fraction) of site j is the thermodynamic average:

$$\theta_j = \langle x_j \rangle = \frac{\sum_{i=1}^{2^N} x_j^i \exp\left(-\frac{U^i}{k_B T}\right)}{\sum_{i=1}^{2^N} \exp\left(-\frac{U^i}{k_B T}\right)}, \quad (1)$$

where superscript i indicates protonation state i, U^i is the energy function of state i, defined by

$$U^i = \sum_{j=1}^{N}\left(x_j^i b_j + \frac{1}{2}\sum_{k\neq j}^{N}(q_j + x_j^i)(q_k + x_k^i)W_{jk}\right),$$

with $b_j = -2.303 k_B T(\mathrm{pK}_{\mathrm{intr,j}} - \mathrm{pH})$, $\mathrm{pK}_{\mathrm{intr,j}}$ is the intrinsic pKa value of the site j, q_j, and q_k is the fixed charge values of the fully unprotonated sites j and k, respectively, W_{jk} is the interaction between the charged sites j and k. The protonation probability determines the average charge state at site j. For a single conformation, the N-component vector $\theta = (\theta_1, \theta_2, \ldots, \theta_N)$ of protonation probabilities (the state vector of protonation) characterizes entirely the thermodynamic average of the charge state of the protein, because the spatial distribution of partial atomic charges of nontitratable groups is fixed. The relative distance value of two vectors θ^A and θ^B can describe the similarity of the electrostatics of two protonation states A and B of the protein, defined by

$$\Delta\theta\% = \frac{100 \times \|\theta^B - \theta^A\|}{\|\theta^A\|}\% \quad (2)$$

We also used another index to characterize the charge state of a protein, the average number of associated protons with a protein $\langle p \rangle$, which is the sum of the protonation probabilities of all titratable sites, as

$$\langle p \rangle = \sum_{j=1}^{N}\theta_j \quad (3)$$

This can be obtained by considering vector $\mathbf{x}$ and Eq. 1. Because other partial charges of atoms are fixed, this quantity determines the final value of the net charge of the protein at given conditions.

The program *multiflex* from MEAD computer program suite (Bashford and Gerwert, 1992; Bashford, 1997) and *Karlsberg* (Rabenstein et al., 2000), an improved version of the MCTI program (Beroza et al., 1991), were employed for calculation of electrostatics and Monte Carlo sampling of protonated states, respectively. The *Karlsberg* program is freely available under the GNU public license from our web server (http://lie.chemie.fu-berlin.de/karlsberg/). Combining these two procedures, the protonation probability θ_j for site j in Eq. 2 was obtained. The program *multiflex* uses a finite difference approach to solve the Poisson-Boltzmann equation to obtain the electrostatic potential, by taking dielectric constants $\epsilon_p = 4$ in the molecular interior and temperature-dependent ϵ_s in the solvent-accessible region. To account for the temperature dependence of ϵ_s, we assume that it is similar to that of the static dielectric constant of water determined experimentally (Eisenberg and Kauzmann, 1969). The ionic strength was set to zero. We have verified that the fusion activity is preserved at very low ionic strength (K. Ludwig and A. Herrmann, unpublished results). In the computation of the electrostatic potential, the finite difference lattice was set as a cubic box. Its edge length was determined by the maximal projection value of the whole protein structure on an axis of the actually used Cartesian frame (x, or y, or z axis) by setting the edge length equal to 125% of the value. Then, two focusing steps where the first with 1.0 Å spacing, the second with 0.25 Å spacing were used to obtain results of sufficient accuracy. To calculate the protonation probability θ_j, 10,000 protonation states for a titratable site j were sampled by the Monte Carlo procedure in the *Karlsberg* program. The standard deviation was less than 0.01 protons for each individual titratable site.

EXPERIMENTAL METHOD AND MATERIALS

Proteinase K sensitivity of HA

Influenza virus X31 was grown for 48 h in the allantoic cavity of 11-day-old embryonated hen eggs. The allantoic fluid was collected and cell debris

TABLE 1 Numbers of proton and charge of HA1 (aa 16-328) and HA2 polypeptide chain (aa 1-134) with assumed protonated side chains according to the standard pKa values of amino acids

Titratable residues	HA1 chain			HA2 chain		
	N_R	N_P	N_C	N_R	N_P	N_C
ARG	15	15	15	6	6	6
ASP	17	0	−17	8	0	−8
GLU	9	0	−9	18	0	−18
HIS	6	0	0	3	0	0
LYS	15	15	15	9	9	9
TYR	10	10	0	3	3	0
Total	72	40	4	47	18	−11

N_R, number of residues in the respective sequence; N_P, total number of protons; N_C, resulting number of charge (unit in $+e$).

was removed by a low speed spin (880 × *g* for 30 min). The virus was pelleted by spinning the allantoic fluid at 95,000 × *g* for 90 min. The pellet was resuspended in PBS (pH 7.4) and homogenized with a Teflon-coated homogenizer. Probing of the conformational change by proteinase K digestion was done as described for influenza virus X-117 A/Beijing/H3/N2 by Carr et al. (1997) with modifications, and 500-μl virus samples (0.1 mg of virus protein/ml) were incubated for 15 min in 5.8 mM PBS under experimental conditions (variation of pH and temperature). In a typical experiment, an incubation temperature was selected and samples were incubated at various pH values. Subsequent to neutralization (pH 7.4) by addition of appropriate amounts of 0.5 M Tris buffer (pH 8.0), samples were digested with proteinase K (30 μg per 500 μl sample) for 3–4 h at room temperature. Proteins and respective fragments were separated by 12% polyacrylamide gels under nonreducing conditions and stained with Coomassie brilliant blue R250. The intensity of the HA-band was taken from densitometric scans of the gels. For comparison of experiments, the intensity was normalized to the intensity of the band corresponding to the nucleoprotein (NP) according to

$$I_{\mathrm{rel}} = \frac{I(HA) - I(B_{\mathrm{HA}})}{I(NP) - I(B_{\mathrm{NP}})}, \tag{4}$$

with I(HA) and I(NP) being the intensity of the HA and NP band, respectively, and $I(B_{HA})$ and $I(B_{NP})$ the intensity of the respective background. The relative amount of cleaved HA, α, was calculated by

$$\alpha = \frac{I_{\mathrm{rel}}}{I_{\mathrm{rel}}^{\mathrm{max}}}, \tag{5}$$

where I_{rel}^{max} is the normalized intensity for the uncleaved HA observed for the highest pH chosen at a given temperature.

RESULTS

Net charges of HA components

To understand the consequences of protonation for the charge and, eventually, for the stability of the HA1 domain at low pH, we first characterized the net charges of the HA components at neutral pH. In Table 1 the numbers of protons and of the corresponding charges of the HA1 chain (amino acids (aa) 16–328) and HA2 chain (aa 1–134) of the ectodomain are given assuming that all the titratable sites

TABLE 2 Average number of protons associated with components of HA ectodomain at pH 7.3 and 300 K

Titratable residues	Average number of associated protons		
	HA1 subunit	HA1 domain*	HA2 domain†
ARG	15.00	44.92	18.00
ASP	00.00	0.00	3.92
GLU	00.00	0.01	8.09
HIS	0.17	3.27	4.31
LYS	14.95	43.94	27.00
TYR	9.98	29.82	9.00
Total	40.10	121.96	70.32

*Trimeric HA1 domain in the absence of HA2.
†Trimeric HA2 domain in the absence of HA1, providing exposure to solvent.

are protonated or unprotonated according to the standard pKa values of amino acids at neutral pH (e.g., see Table 4.2 in Zubay, 1998); lysine, arginine, and tyrosine residues are protonated whereas histidine, aspartic acid, and glutamic acid residues are unprotonated. Thus, HA1 and HA2 possess a net charge of $+4e$ and $-11e$, respectively. However, this assumed protonation state does not consider the three-dimensional structure of the HA ectodomain. Therefore, we have constructed the all-hydrogen-atoms structure of the HA1 monomer, of the trimeric HA1 domain, and of the trimeric HA2 domain from the known x-ray structure of the ectodomain of HA from X31 (Wilson et al., 1981) (see Theory and Modeling Methods). For those structures, the average number of protons associated with titratable sites at pH = 7.3 and T = 300 K was calculated according to Eq. 1 (Table 2). Comparing the results with those in Table 1, it is obvious that the number of protons in the HA1 chain defined by standard pKa values of amino acids (Table 1) is very similar to that of the HA1 subunit in the real three-dimensional conformation. Likewise, the total number of associated protons of three individual HA1 subunits is found to be almost identical to that of the HA1 domain in the trimeric configuration (absence of HA2). This implies that at pH 7.3 and 300 K, the protonation state of a HA1 monomer is similar to that in the trimeric HA1 domain (see Table 2). As mentioned, most parts of the HA2 domain in the neutral pH conformation of the HA ectodomain are shielded from the solvent medium and are unable to undergo protonation reaction with solvent; thus, in principle the net charge of the HA2 domain is independent of pH. Nevertheless, we also calculated via Eq. 1 its average number of associated protons supposing this domain is exposed entirely to the solvent (absence of HA1 domain). The calculated number of net charge is $\sim -16e$ in the trimeric HA2 domain. Comparing with three individual HA2 chains in the assumed protonation state (Table 1), there is a change of the average net charge number from $-33e$ ($-11e$ per HA2 chain) to $\sim -16e$ due to protonated side chains of aspartic acid, glutamic acid, and histidine residues. Of course, because the actual HA2 domain is not exposed to solvent, it is

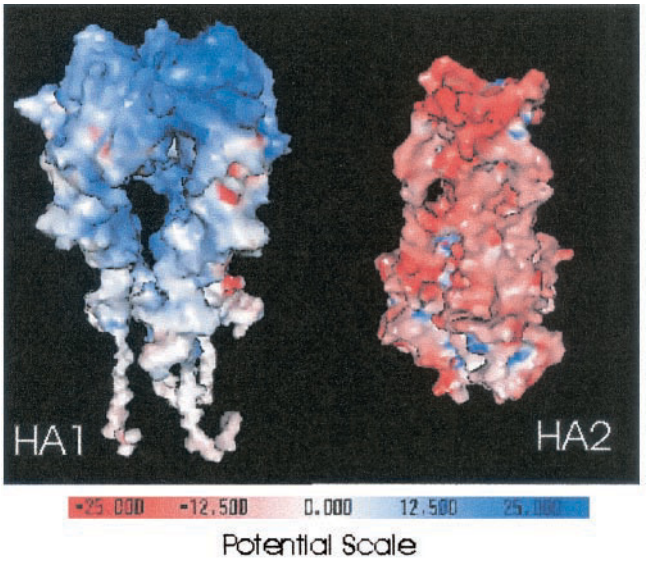

FIGURE 2 Surface electrostatic potential of HA1 domain and HA2 domain with GRASP. Electrostatic potential is color-coded using a sliding scale indicated in the lower part of the figure (unit in k_BT/e). Red represents negative electrostatic potential, blue represents positive electrostatic potential, and white is neutral.

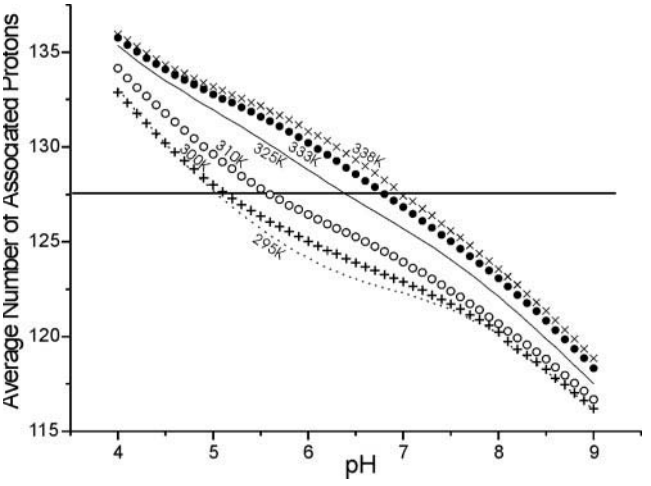

FIGURE 3 Average numbers of associated protons with the HA1 domain at various pH-temperature conditions. The straight line in the figure indicates the value of the average number of associated protons at pH = 5.1 and T = 300 K, which is 127.63. Using this line, the pH values, where the HA1 domain possesses similar values of average numbers of associated protons at temperatures T = 295 K, 310 K, 325 K, 333 K, and 338 K, are shown at pH = 5.0, 5.7, 6.5, 6.9, and 7.1, respectively.

difficult to predict its exact value of net charge. However, as seen in Table 1, this domain consisting of three HA2 chains contains in total 24 aspartic acid and 54 glutamic acid residues that can give rise to a large negative charge if they are unprotonated. Indeed, only a few of them are protonated even if the whole domain is exposed to solvent. Although, in this case, other residues are essentially in the protonated form and possess net positive charge, the net charge of the whole domain is still $-16e$ (see Table 2). Therefore, it is reasonable to conclude that the net charge of HA2 domain of the native, pH-neutral form of the HA ectodomain is basically negative.

Fig. 2 demonstrates the surface electrostatic potential of the HA1 domain and of the HA2 domain produced with the GRASP program (Nicholls, 1992). The HA2 domain, in particular the distal part, is locally enriched by negative charges, whereas the corresponding contact position of the HA1 domain is enriched by positive charges. The results indicate that in the HA ectodomain at neutral pH, the electrostatic force between either three subunits of HA1 or of HA2 is repulsive; however, that between HA1 and HA2 domains is attractive. Moreover, because the net charge in the HA1 domain is positive, enhanced protonation of this domain will lead to an even more positive charge that will give rise to an additional electrostatic repulsion between the three subunits of the HA1 domain.

Number of associated protons with HA1 domain

Because the conformational change of HA triggering fusion is dependent on the pH as well as on the temperature (see below and Carr et al., 1997), we have calculated the protonation of the HA1 domain at various pH values and temperatures. Although we are aware that part of the HA2 domain could be accessible to solvent, in the computations, we did not consider the HA2 domain for the following reasons. First, the residues on the surface of HA1 domain do not contact residues of the HA2 domain but are rather far away from them. Thus, it is reasonable to assume that the protonation of the titratable residues on the HA1 surface is mainly influenced by other residues of HA1 and that effects from HA2 domain may be negligible. Second, a practical viewpoint is that the whole HA ectodomain is very large and requires intensive computations. The exclusion of the HA2 domain from computation allows an easier and more effective computational handling, because the total numbers of atoms and titratable residues needed to be considered decrease significantly. Although computation of the whole ectodomain may provide a more accurate result, we are convinced that, also based on the first reason (see above), conclusions similar to that by considering only HA1 will be obtained. The agreement between theoretical and experimental results (see below) is a strong indication for the validity of our approach.

In Fig. 3 the average number of protons associated with the HA1 domain is shown as the function of the pH value ranging from 4.0 to 9.0. At room temperature, typically, the fusion potential of HA is activated at an acidic pH between pH 5 and pH 6 (Maeda and Ohnishi, 1980; Huang et al., 1981; White et al., 1982). In particular, the fusion maximum of X31 is induced at the lower pH limit of about pH 5 (Korte et al., 1997). The average number of protons associated with

TABLE 3 Difference values of the average numbers of associated protons of some residues of the HA1 domain at pH 5.1 and 300 K from those at pH 7.3 and 300 K

Titratable residues	HA1 chains			HA1 domain
	A	C	E	
GLU35	0.25	0.19	0.17	
LYS259	0.09	0.10	0.10	
LYS299	0.12	0.12	0.11	
HIS17	0.44	0.45	0.41	
HIS75	0.47	0.43	0.42	
Total	1.37	1.29	1.21	3.87

In 2HMG, the three identical HA1 chains are labeled as A, C, and E, respectively. Each chain consists of 328 amino acid residues (1-328).

TABLE 4 Conformational change of HA of X31 from the native conformation to a proteinase K-sensitive state

Temperature (K)	pH	α
310.15	5.72	0.39
	5.91	0.86
	6.20	1.02
	6.60	1.16
	7.31	1.07
	7.49	1.00
320.15	6.20	0.51
	6.60	0.80
	7.04	0.80
	7.49	1.00
325.15	5.75	0.0
	5.91	0.06
	6.20	0.09
	6.60	0.76
	7.31	1.06
	7.49	1.16
	7.94	1.00
330.15	6.20	0.28
	6.60	0.43
	7.04	1.11
	7.49	0.97
	7.94	1.00

The relative amount of proteolytically cleaved HA α at given temperatures and pH values (for details see Experimental Method and Materials).

the HA1 domain at 300 K and pH 5.1 corresponding to ~127.6 (see straight line in Fig. 3) is enhanced with respect to nonfusogenic conditions (pH 7.3, 300 K). Following the hypothesis that the enhanced protonation of the HA1 subunit plays an essential role in the conformational change, we have studied how this degree of protonation depends on pH and temperature.

In the room temperature range (295–300 K) the pH value with a similar average number of associated protons of ~127.6 does not depend greatly on temperature and is ~5.1 (Fig. 3). However, by shifting the temperature to higher values, the same average protonation of ~127.6 protons is obtained at less acidic pH. At temperatures of 310 K, 325 K, 333 K, and 338 K, the respective pH corresponding to the average of ~127.6 associated protons is 5.7, 6.5, 6.9, and 7.1, respectively. Thus, at these conditions, the electrostatic state of the HA1 domain is almost similar. To confirm the similarity of the electrostatic states at those pH-temperature points, we also compared the difference between the state vectors of protonation (Eq. 2), using the state vector at (pH 5.0, $T = 295$ K) as the reference vector θ^A. The relative distance values $\Delta\theta$% of the state vectors at pH 5.1, $T = 300$ K; pH 5.7, $T = 310$ K; pH 6.5, $T = 325$ K; pH 6.9, $T = 333$ K; and pH 7.1, $T = 338$ K to the reference vector are 4.3%, 4.9%, 5.7%, 6.9%, and 7.1%, respectively. These low values also strongly suggest that the electrostatic state of HA1 domain is almost identical at the various selected pH-temperature points. In comparison with the value of the trimeric HA1 domain at pH 7.3 and 300 K (see Table 2), on average, there is an increase of about six associated protons at the given pH-temperature points. Which are the essential residues contributing to this increase? To address this question, we have calculated the difference between the average number of associated protons of individual residues at fusogenic and nonfusogenic conditions. For example, in Table 3 the respective difference between pH 5.1, 300 K, and pH 7.3, 300 K, are shown. Only those residues are listed for which the absolute difference values are greater than 0.10, at least in one of HA1 chains. These residues can be viewed as the residues with the largest contribution to the increase in average number of associated protons. However, these residues do account only for about half of the total increase of protonation of the whole ectodomain (about six protons). This implies that the increase of associated protons at low pH cannot be simply attributed to the protonation of a few of residues of the HA1 domain. To confirm the role of distinct amino acids listed in Table 3 for protonation, studies of site-directed mutagensis of HA are currently underway.

Proteinase K sensitivity of HA

We have investigated the conformational change of the HA ectodomain as a function of pH and temperature. The rationale for these experiments was to probe whether this dependence correlates with that of protonation of $\langle p \rangle \approx 127.6$ of the HA1 domain (see above). The conformational change of the HA ectodomain was assessed by a proteolysis assay using proteinase K. The resistance of HA in the native conformation to digestion by the enzyme is lost in the acid-induced conformation (Doms et al., 1985) that can be visualized by polyacrylamide gel electrophoresis. In Table 4 and Fig. 4 the data are summarized. As can be seen in Fig. 4, with increasing temperature, the pH at which the conformational change occurred is shifted to higher values in agreement with previous studies (Ruigrok et al., 1986a; Carr et al., 1997). Due to the size of the increment of pH and temperature, the transition from the native conformation to the protease-sensitive state is not sharply defined. Remarkably, the pH and temperature dependence of the conforma-

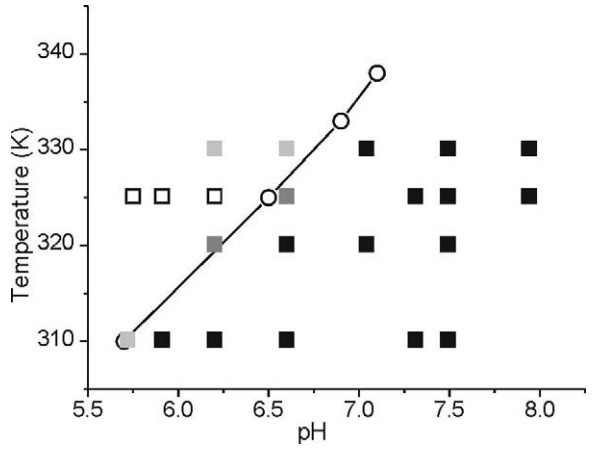

FIGURE 4 Conformational change of HA of X31 from the native conformation to a proteinase K-sensitive state as a function of pH and temperature. The conformational transition is shifted to higher pH thresholds with increasing temperatures. The relative amount of cleaved HA α (see Table 4) is shown in dependence of pH and temperature. For graphic presentation, values with $\alpha \geq 0.8$ are considered to represent the proteolysis-resistant conformation (*solid bars*), with $\alpha \leq 0.2$ as the proteolysis-sensitive state (*open bars*), and values with $0.5 < \alpha < 0.8$ and $0.2 < \alpha \leq 0.5$ reflect the region of the transition (*gray* and *light gray bars*, respectively). Open circles and line correspond to the predicted pH-temperature dependence of the specific degree of protonation of the HA1 domain shown in Fig. 3 (see *straight line*). For further explanation, see Results.

tional change is almost similar to that of the calculated average number of ~127.6 associated protons with HA1 domain as indicated by the open circles and line in Fig. 4.

DISCUSSION

Protonation and conformational change of HA

To enable the transition of HA2 into the coiled-coil, rod-like-shaped conformation the tight contact between HA monomers in the ectodomain has to be destabilized. Because at physiological temperatures the conformational change of HA requires an acidic pH, protonation of the ectodomain is essential for the destabilization, in particular of the HA1 subunits, which in contrast to the HA2 subunits are not shielded from the aqueous medium. Therefore, we analyzed the protonation of the HA1 subunits. As expected, at typical conditions for fusion of influenza X31, at pH 5.1 and a temperature of ~300 K, we found an increase of the protonation of the HA1 subunits. The essential role of protonation for the conformational change of HA is underlined by our detailed analysis and comparison of the pH and temperature dependence of the conformational change of HA and of the degree of HA1 protonation. By assessing the conformational change by proteinase K digestion, we found in agreement with previous studies (Ruigrok et al., 1986a; Carr et al., 1997) that raising the temperature shifts the pH threshold for triggering the conformational change to less acidic or even neutral/basic pH values. As already shown by Carr et al. (1997) for influenza virus X117, which is also of subtype H3, the conformational changes at certain pH-temperature conditions are indistinguishable.

As expected and confirmed by our results, decreasing pH is correlated with increasing protonation. Now, we found a close quantitative correlation between the pH threshold (including neutral pH) of the conformational change at a given temperature and the average protonation of the HA1 domain at those conditions (see Fig. 3). The protonation state was similar ($\langle p \rangle \approx 127.6$) at all threshold points. Taking the average protonation as a parameter characterizing the electrostatic state of a protein (domain) we suggest that at the various temperature-dependent pH thresholds of the conformational change the electrostatic interaction between HA1 subunits is similar. Because protonation enhances the positive net charge of each HA1 subunit and, by that, the repulsive component, the stability of the ectodomain may become reduced. In particular, the tight contact of HA1 subunits could be affected, which may lead to a sideward relocation of the HA1 subunits releasing constraints of other conformational alterations. This provides a theoretical basis and explanation for the puzzled observations on conformational changes of HA occurring at higher and neutral pH (see below). Furthermore, a weakened attraction between HA subunits may facilitate not only a relocation of the subunits but also a conformational change.

We want to point out that calculations of forces and average protonation are strictly linked to the native conformation of the HA ectodomain known from the x-ray structure. Any change of the arrangement of the ectodomain affects forces and protonation. However, this does not impair the value of our approach, because initially the force-balanced conformation of the native, pH-neutral conformations has to be disturbed.

Model for early steps of HA conformational change

An essential step of the conformational change of the HA ectodomain to a fusion active state is the rearrangement of the distal HA1 domain. This is supported by studies employing chemical cross-linking, antibody binding, proteolysis, electron microscopy, and site-specific mutation (Graves et al., 1983; Webster et al., 1983; Doms et al., 1985; Ruigrok et al., 1986b, 1988; White and Wilson 1987; Daniels et al., 1987; Godley et al., 1992; Kemble et al., 1992; Böttcher et al., 1999). In particular, inhibition of fusion by intermonomer disulfide bonds in the distal domain of HA1 indicates that a sideward relocation of the HA1 distal globular domains is a prerequisite for the genesis of a fusion active conformation (Kemble et al., 1992). Direct evidence for a rearrangement of the HA1 ectodomain is given by our study on the three-dimensional structures of the complete hemagglutinin of influenza virus A/Japan/305/57 (H2) in its native (neutral-pH) and membrane fu-

sion-competent (low-pH) form by electron cryo-microscopy at a resolution of 10 Å and 14 Å, respectively (Böttcher et al., 1999). Significant distinctions between both structures are a flattening of the top of the distal HA1 domains and a continuous central cavity through the whole trimer of the fusion-competent conformation. These studies strongly imply that the rearrangement of and displacement within the distal HA1 domain is the initial step of the conformational change, upstream of the coiled-coil formation of the HA2 subunits. Such a displacement in the HA1 domain can be triggered by repulsive force. We suggest that an enhanced association of protons with the HA1 domain may cause a weakened attraction between the HA1 subunits. An enhanced repulsion may affect only the organization of distinct parts of the HA1 domain but not the whole HA1 subunits. Indeed, regardless of the significant alterations of the HA1 distal domain in its fusion-competent form detected by cryo-electron microscopy (see above and Shangguan et al., 1998; Korte et al., 1999), the overall shape of the trimeric ectodomain at neutral pH was preserved.

The reorganization of the HA1 domain and the formation of a central cavity of the fusion-competent structure leave space and freedom for the formation of the extended coiled-coil structure of the HA2 subunits by the proposed spring-loaded mechanism (Carr and Kim, 1993). The loop region between the two α-helices of the HA2 subunit of the neutral pH form has been found to remain highly flexible at low pH (Kim et al., 1996). Both the flexibility of the loop region and the central cavity may facilitate the relocation of the coiled coil with the fusion peptides toward the tip of the ectodomain, the site of the target membrane. Further reorganization and bending of the ectodomain by the formation of an antiparallel helices bundle (Bullough et al., 1994; Chen et al., 1999) leads to a close contact between the fusion sequence and the transmembrane domain of HA. This may facilitate or mediate a close approach of the fusion peptide to the membrane preceding membrane fusion.

According to the model, the reorganization of the HA1 domain requires protonation and, thus, under natural conditions an acidification of the viral environment. Although it has been shown that the transition of the loop region of HA2 into a helix and the subsequent formation of the trimeric coiled-coil motif occurs also at neutral pH (Carr and Kim, 1993; Chen et al., 1995), it remains open whether other steps of the conformational change of the ectodomain require an acidic pH at physiological temperatures. However, the close correlation between the calculated protonation of the HA1 domain and the predicted and the experimentally observed temperature- and pH-dependent thresholds of the dissociation of HA1 subunits leads to the working hypothesis that only the dissociation of the HA1 subunits requires an acidic pH. Once this rearrangement has been triggered, other alterations of the ectodomain leading to a fusion-competent structure will spontaneously proceed, which is consistent with the view of the native conformation as a metastable state (Carr et al., 1997). The tight association of the HA1 domains at neutral pH acts as a clamp, preventing the formation of the coiled-coil and the exposure of the fusion sequence.

Several studies suggest that an extended, triple-stranded rod-shaped α-helical coiled-coil represents a common structural and functional motif of fusion proteins of various enveloped viruses (see a review in Skehel and Wiley, 1998), implying a common fusion mechanism. Comparison with other viral fusion-mediating proteins suggests that such a clamp may resemble also a typical structural feature. To release the clamp, different strategies have evolved. Although for HA, low pH may release the clamp by a mechanism suggested here, other enveloped viruses do not need acidic pH for that. For instance, for the fusion-mediating gp41/gp120 protein of HIV, gp120 and its interaction with gp41 acts as a clamp preventing the formation of the coiled coil in the gp41 subunit. The interaction of gp120 with distinct receptors on the host cell plasma membrane triggers a conformational change of gp120 turning down its clamp function (Doms and Moore, 2000). Subsequently, the coiled-coil motif is formed in the gp41 subunit. Because the latter proceeds at neutral pH, a further implication of this comparison is that the formation of the coiled-coil of HA2 may not require low pH.

Special thanks to Peter Vagedes, Dragan Popovic, and Björn Rabenstein for assistance in using the related programs and to Kai Ludwig, Britta Schroth-Diez, Thomas Korte, and Christine Kozerski for helpful comments.

This work was supported by grants of the Deutsche Forschungsgemeinschaft (A.H. and E.-W.K.); Q.H. was supported by a scholarship from DAAD (German Academic Exchange Service).

REFERENCES

Bashford, D. 1997. An object-oriented programming suite for electrostatic effects in biological molecules. *Lect. Notes Comp. Sci.* 1343:233–240.

Bashford, D., and K. Gerwert. 1992. Electrostatic calculations of the pKa values of ionizable groups in bacteriorhodopsin. *J. Mol. Biol.* 224: 473–486.

Bashford, D., and M. Karplus. 1991. Multi-site titration curves of proteins: an analysis of exact and approximate methods for their calculation. *J. Phys. Chem.* 95:9556–9561.

Beroza, P., D. R. Fredkin, M. Y. Okamura, and G. Feher. 1991. Protonation of interacting residues in a protein by a Monte Carlo method: application to lysozyme and the photosynthetic reaction center. *Proc. Natl. Acad. Sci. U.S.A.* 88:5804–5808.

Böttcher, C., K. Ludwig, A. Herrmann, M. van Heel, and K. Stark. 1999. Structure of influenza haemagglutinin at neutral and at fusogenic pH by electron cryo-microscopy. *FEBS Lett.* 463:255–259.

Brooks, B. R., R. E. Bruccoleri, B. D. Olafson, D. J. States, S. Swainathan, and M. Karplus. 1983. CHARMM: a program for macromolecular energy, minimization, and dynamics calculations. *J. Comp. Chem.* 4:187–217.

Bullough, P., F. M. Hughson, J. J. Skehel, and D. C. Wiley. 1994. Structure of influenza hemagglutinin at the pH of membrane fusion. *Nature.* 371:37–43.

Carr, C. M., C. Chaudhry, and P. S. Kim. 1997. Influenza hemagglutinin is spring-loaded by a metastable native conformation. *Proc. Natl. Acad. Sci. U.S.A.* 94:14306–14313.

Carr, C. M., and P. S. Kim. 1993. A spring-loaded mechanism for the conformational change of influenza hemagglutinin. *Cell.* 73:823–832.

Chen, J., J. J. Skehel, and D. C. Wiley. 1999. N- and C-terminal residues combine in the fusion-pH influenza hemagglutinin HA2 subunit to form an N cap that terminates the triple-stranded coiled coil. *Proc. Natl. Acad. Sci. U.S.A.* 96:8967–8972.

Chen, J., S. A. Wharton, W. Weissenhorn, L. J. Calder, F. M. Hughson, J. J. Skehel, and D. C. Wiley. 209. 1995. A soluble domain of the membrane-anchoring chain of influenza virus hemagglutinin (HA2) folds in *Escherichia coli* into the low-pH-induced conformation. *Proc. Natl. Acad. Sci. U.S.A.* 92:12205–12212.

Daniels, R. S., S. Jeffries, P. Yates, G. C. Schild, G. N. Rogers, J. C. Paulson, S. A. Wharton, A. R. Douglas, J. J. Skehel, and D. C. Wiley. 1987. The receptor binding and membrane fusion properties of influenza virus variants selected using anti-haemagglutinin monoclonal antibodies. *EMBO J.* 6:1459–1465.

Doms, R. W., A. Helenius, and J. White. 1985. Membrane fusion activity of influenza virus hemagglutinin. *J. Biol. Chem.* 260:2973–2981.

Doms, R. W., and J. P. Moore. 2000. HIV-1 membrane fusion: targets of opportunity. *J. Cell Biol.* 151:F9–F13.

Eckert, D. M., and P. S. Kim. 2001. Mechanisms of viral membrane fusion and its inhibition. *Annu. Rev. Biochem.* 70:777–810.

Eisenberg, D., and W. Kauzmann. 1969. The Structure and Properties of Water. Oxford University Press, London. 189–191.

Godley, L., J. Pfeifer, D. Steinhauer, B. Ely, G. Shaw, R. Kaufmann, E. Suchanek, C. Pabo, J. J. Skehel, D. C. Wiley, and S. Wharton. 1992. Introduction of intersubunit disulfide bonds in the membrane-distal region of the influenza hemagglutinin abolished membrane fusion activity. *Cell.* 68:635–645.

Graves, P. N., J. L. Schulman, J. F. Young, and P. Palese. 1983. Preparation of influenza virus subviral particles lacking the HA1 subunit of hemagglutinin: unmasking of cross-reactive HA2 determinants. *Virology.* 126:106–116.

Huang, R. T. C., R. Rott, and H.-D. Klenk. 1981. Influenza virus causes hemolysis and fusion of cells. *Virology.* 110:243–247.

Kemble, G. W., D. L. Bodian, J. Rose, I. A. Wilson, and J. M. White. 1992. Intermonomer disulfide bonds impair the fusion activity of influenza virus hemagglutinin. *J. Virol.* 66:4940–4950.

Kim, C.-H., J. C. Macosko, Y. G. Yu, and Y.-K. Shin. 1996. On the dynamics and conformation of the HA2 domain of the influenza virus hemagglutinin. *Biochemistry.* 35:5339–5365.

Korte, T., K. Ludwig, F. P. Booy, R. Blumenthal, and A. Herrmann. 1999. Conformational intermediates and fusion activity of influenza hemagglutinin. *J. Virol.* 73:4567–4574.

Korte, T., K. Ludwig, M. Krumbiegel, D. Zirwer, G. Damaschun, and A. Herrmann. 1997. Transient changes of the conformation of hemagglutinin of influenza virus at low pH detected by time-resolved circular dichroism spectroscopy. *J. Biol. Chem.* 272:9764–9770.

MacKerell, A. D., Jr., D. Bashford, M. Bellot, R. L. Dunbrack, Jr., J. D. Evanseck, M. J. Field, S. Fischer, J. Gao, H. Guo, S. Ha, D. Joseph-McCarthy, L. Kuchnir, K. Kuczera, F. T. K. Lau, C. Mattos, S. Michnick, T. Ngo, D. T. Nguyen, B. Prodholm, W. E. Reiher, I. I. I., B. Roux, M. Schlenkrich, J. C. Smith, R. Stote, J. Straub, M. Watanabe, J. Wiórkiewicz-Kuczera, D. Yin, and M. Karplus. 1998. All-atom empirical potential for molecular modeling and dynamics studies of proteins. *J. Phys. Chem. B.* 102:3586–3616.

Maeda, T., and S. Ohnishi. 1980. Activation of influenza virus by acidic media causes hemolysis and fusion of erythrocytes. *FEBS Lett.* 122: 283–287.

Nicholls, A. 1992. GRASP: Graphical Representation and Analysis of Surface Properties. Columbia University, New York.

Qiao, H., S. L. Pelletier, L. Hoffman, J. Hacker, R. T. Armstrong, and J. M. White. 1998. Specific single or double proline substitutions in the "spring-loaded" coiled-coil region of the influenza hemagglutinin impair or abolish membrane fusion activity. *J. Cell Biol.* 141:1335–1347.

Rabenstein, B., G. M. Ullmann, and E. W. Knapp. 2000. Electron transfer between the quinones in the photosynthetic reaction center and its coupling to conformational changes. *Biochemistry.* 39:10487–10496.

Ramalho-Santos, J., and M. C. P. de Lima. 1998. The influenza virus hemagglutinin: a model protein in the study of membrane fusion. *Biochem. Biophys. Acta.* 1376:147–154.

Ruigrok, R. W. H., A. Aitken, L. J. Calder, S. R. Martin, J. J. Skehel, S. A. Wharton, W. Weis, and D. C. Wiley. 1988. Studies on the structure of influenza virus hemagglutinin at the pH of membrane fusion. *J. Gen. Virol.* 69:2785–2795.

Ruigrok, R. W. H., S. R. Martain, S. A. Wharton, J. J. Skehel, P. M. Bayley, and D. C. Wiley. 1986a. Conformational changes in the hemagglutinin of influenza virus which accompany heat-induced fusion of virus with liposomes. *Virology.* 155:484–497.

Ruigrok, R. W. H., N. G. Wrigley, L. J. Calder, S. Cusack, S. A. Wharton, E. B. Brown, and J. J. Skehel. 1986b. Electron microscopy of the low pH structure of influenza virus hemagglutinin. *EMBO J.* 5:41–49.

Shangguan, T., D. P. Siegel, J. D. Lear, P. H. Axelsen, D. Alford, and J. Bentz. 1998. Morphological changes and fusogenic activity of influenza virus hemagglutinin. *Biophys. J.* 74:54–62.

Skehel, J. J., and D. C. Wiley. 1998. Coiled coils in both intracellular vesicles and viral membrane fusion. *Cell.* 95:871–874.

Ullmann, G. M., and E. W. Knapp. 1999. Electrostatic models for computing protonation and redox equilibria in proteins. *Eur. Biophys. J.* 28:533–551.

Webster, R. G., L. E. Brown, and D. C. Jackson. 1983. Changes in the antigenicity of the hemagglutinin molecules of H3 influenza virus at acid pH. *Virology.* 126:587–599.

White, J., K. Martin, and A. Helenius. 1982. Cell fusion by Semliki forest, influenza and vesicular stomatitis viruses. *J. Cell. Biol.* 89: 674–679.

White, J. M., and I. A. Wilson. 1987. Anti-peptide antibodies detect steps in a protein conformational change: low pH activation of the influenza virus hemagglutinin. *J. Cell Biol.* 105:2887–2896.

Wilson, I. A., J. J. Skehel, and D. C. Wiley. 1981. Structure of the haemagglutinin membrane glycoprotein of influenza virus at 3 Å resolution. *Nature.* 289:366–373.

Zubay, G. 1998. Biochemistry. Wm. C. Brown Publishers, Dubuque, IA.